Title: Tunable Elastomer Materials With Vascular Tissue-Like Rupture Mechanics Behavior

Authors: Andrea Corti[a], Tariq Shameen[a,1], Shivang Sharma[a,1], Annalisa De Paolis PhD[a], Luis Cardoso PhD[a]

Affiliations: [a]City College of the City University of New York, Department of Biomedical Engineering, New York, NY 10029, USA
Present address: [1]Memorial Sloan Kettering Cancer Center, New York, NY 10065, USA, [2]Rimsys Regulatory Management Software, Pittsburgh, PA 15212, USA

Contact email: *Cardoso@ccny.cuny.edu*

Authors Contribution Statement

Andrea Corti: Conceptualization, Methodology, Data Curation, Validation, Writing-original draft; **Tariq Shameen**: Methodology, Data Curation, Validation; **Shivang Sharma**: Methodology, Data Curation; **Annalisa De Paolis***:* Methodology, Data Curation, Validation; **Luis Cardoso**: Conceptualization, Methodology, Supervision, Writing-review & editing, Funding acquisition.

Abstract

Purpose: Laboratory models of human arterial tissues are advantageous to examine the mechanical response of blood vessels in a simplified and controllable manner. In the present study, we investigated three silicone-based materials for replicating the mechanical properties of human arteries documented in the literature.
Methods: We performed uniaxial tensile tests up to rupture on Sylgard184, Sylgard170 and DowsilEE-3200 under different curing conditions and obtained their True (Cauchy) stress-strain behavior and Poisson's ratios by means of digital image correlation (DIC). For each formulation, we derived the constitutive parameters of the 3-term Ogden model and designed numerical simulations of tubular models under a radial pressure of 250mmHg.
Results: Each material exhibits evident non-linear hyperelasticity and dependence on the curing condition. Sylgard184 is the stiffest formulation, with the highest shear moduli and ultimate stresses at relative low strains (μ_{184}=0.52-0.88MPa, σ_{184}=15.90-16.54MPa, ε_{184}=0.72-0.96). Conversely, Sylgard170 and DowsilEE-3200 present significantly lower shear moduli and ultimate stresses that are closer to data reported for arterial tissues (μ_{170}=0.33-0.7MPa σ_{170}=2.61-3.67MPa, ε_{170}=0.69-0.81; μ_{dow}=0.02-0.09MPa σ_{dow}=0.83-2.05MPa, ε_{dow}=0.91-1.05). Under radial pressure, all formulations except DowsilEE-3200 at 1:1 curing ratio undergo circumferential stresses that remain in the elastic region with values ranging from 0.1 to 0.18MPa.
Conclusion: Sylgard170 and DowsilEE-3200 appear to better reproduce the rupture behavior of vascular tissues within their typical ultimate stress and strain range. Numerical models demonstrate that all three materials achieve circumferential stresses similar to human common carotid arteries (Sommer et al. 2010), making these formulations suited for cylindrical laboratory models under physiological and supraphysiological loading.

Keywords: Laboratory models, Mock vessels, Ultimate Tensile Stress, Sylgard, Dowsil, Uniaxial Tensile Testing

Introduction

Cardiovascular diseases (CVD) have represented the leading cause of death in the last three decades and the rate of mortality has steadily increased since 1990 (Roth et al. 2020; World Health Organization 2020). Unfortunately, this trend is not expected to change any time soon. The underlying pathology of CVD is atherosclerosis, which is initiated by cholesterol build-up beneath the endothelium of artery blood vessels, which ultimately evolves into an atherosclerotic plaque(Burke et al. 2014). The rupture of this plaque can result in major clinical outcomes, including myocardial infarction, sudden coronary death, stroke, transient ischemic attack, and critical limb ischemia. For this reason, intense scientific effort is spent to better understand the biomechanics of the human vascular system. A significant share of this research relies on multiple in-vitro techniques to replicate and predict the behavior of arterial tissues under different types of loading (Macrae, Miller, and Doyle 2016; Holzapfel et al. 2005; Holzapfel, Sommer, and Regitnig 2004; Sommer et al. 2010; Kural et al. 2012; Jankowska, Bartkowiak-Jowsa, and Bedzinski 2015; Maher et al. 2009; Teng et al. 2009). Such mechanical tests can be used to investigate the macroscopic behavior of arteries as well as analyze the effect of microscopic features that may influence the biomechanics of vascular tissue rupture and the stability of atherosclerotic plaques. However, performing these experiments on blood vessels presents several challenges. The specimens require delicate handling, and their manipulation can potentially alter the outcome of the experiments. In addition, it can be difficult to isolate the effect of individual aspects of vessel's morphology and composition on plaques stability given the heterogeneous and multifactorial nature of arterial tissues. Therefore, the development of tissue-mimicking materials with similar mechanical properties as human blood vessels to study the behavior of atheroma-like phantoms with reproducible and tunable mechanical properties comprise an alternative to the challenges posed by experimental testing of blood vessels. The use of a laboratory model reduces the complexity of the problem at hand and allows to better examine the significance of specific factors that may otherwise be very difficult to study.

One of the most adopted elastomers in the field is polydimethylsiloxane (PDMS), in particular the two types Sylgard184 and Sylgard170 (Dow Corning Corporation). These two silicones have a simple manufacturing process, present a nonlinear behavior and Sylgard184 material properties are known to vary with both curing and operational temperatures (Mata, Fleischman, and Roy 2005; Liu et al. 2009; Kim, Kim, and Jeong 2011; Johnston et al. 2014; Choi, Park, and Oh 2014). Sylgard184 is also biocompatible, which makes this silicone a good substrate for cell culture and mechanotransduction studies (Fischer et al. 2017; Hecker et al. 2005; Colombo et al. 2010). The hyperelastic properties of these materials within the low stretch range (30-50% stretch) resemble the typical stress-hardening behavior of soft tissues, which results from stretching the constitutive elastic fibers of the extracellular tissue, in particular collagen (Payan and Ohayon 2017; Fratzl 2008). For this reason, Sylgard184 and Sylgard170 have been previously used to prepare laboratory models of healthy arteries and aortic aneurysm (Colombo et al. 2010; Doyle et al. 2010, 2009). While the mechanical tunability of Sylgard 184 has been extensively investigated (Liu, Sun, and Chen 2009; Liu 2007; Liu et al. 2009; Mata, Fleischman, and Roy 2005; Kim, Kim, and Jeong 2011; Johnston et al. 2014), the studies on mechanical properties of Sylgard170 are scarce. Studies on the behavior of Sylgard170 have only been reported for the mix curing ratio recommended by the provider (Doyle et al. 2009, 2010); however, there exist the potential for tuning its mechanical properties when modifying the base (pre-polymer) to curing agent (cross-linker) ratio. Importantly, the ultimate strength (i.e. maximal stress at rupture) of Sylgard184 seems to be too high compared to that reported for any type of artery, while the ultimate strain seems comparable to that of arterial tissues (Liu et al. 2009; Mata, Fleischman, and Roy 2005; Doyle et al. 2009; Akyildiz, Speelman, and Gijsen 2014; Walsh et al. 2014). This makes Sylgard184 less suited for replicating the rupture mechanism of vascular tissues within their typical stress and strain range to rupture. On the other hand, the encapsulant DowsilEE-3200 (Dow Corning Corporation) appears

to show a significantly lower ultimate strength (0.55MPa, based on the provider's documentation) while maintaining a hyperelastic response under high deformations. Hence, DowsilEE-3200 could be a potential candidate for arterial tissue laboratory models. To the best of our knowledge, there is no literature of a mechanical analysis of DowsilEE-3200 or Sylgard 170 under different curing conditions to develop atheroma-like phantoms that can replicate the biomechanics of rupture of atheromatous plaque tissues.

Therefore, the purpose of this study is to provide an accurate characterization of the material properties of Sylgard184, Sylgard170 and DowsilEE-3200 under different curing formulations by combining uniaxial tensile tests, digital image correlation (DIC) and numerical simulations. This analysis is intended to be used as a reference for future application of these materials as vascular laboratory models to investigate the biomechanics of plaque rupture.

Material and methods

SAMPLES PREPARATION

Samples were manufactured based on 80%-scaled down ASTM D412-Type C geometry to replicate typical dimensions of arterial tissues. Each specimen had a gauge region with a length, width, and thickness of 6.6, 1.2 and 0.6 mm respectively (**Fig.1**). To prepare our samples, we injected the material into a custom-designed molding system consisting of two 0.5in (1.27cm)-thick plates. The bottom plate was carved with a total of 12 sample shapes using a milling machine. The top plate was then used to cover the bottom part and the system was tightly closed by a set of screws and nuts (**Fig.1**). The two plates were made of Polyetherimide, which is an amber-transparent thermoplastic with a glass transition temperature of 217 °C (Kyriacos 2017).

The three elastomer materials are supplied as a two-part kit, consisting of a pre-polymer and a cross-linker (Sylgard184) or PartA and PartB (Sylgard170 and Dowsil EE-3200).
Sylgard184: Samples were prepared using 15:1, 10:1 (recommended by the manufacturer) and 5:1 base-to-curing agent ratios. For each group, the PDMS was thoroughly mixed, degassed for about 30 minutes, poured into the molds, cured at 30 °C for 16 hours and then cured again at 100 °C for 4 hours.
Sylgard170: We tested the material at 1:1 (recommended by the manufacturer), 5:1 and 1:5 Part A-Part B ratios. Samples were prepared following the same protocol as for Sylgard184.
Dowsil EE-3200: For this material, the mixtures considered were 1:1 (recommended by the manufacturer), 1:1.5 and 1:2.5 ratios. The manufacturing process was the same as for the other materials except the final curing temperature was set to 50 °C, as the provider recommends not to heat the material above 60 °C. For every formulation, each ratio between the two mixing parts was considered by weight.

After the curing process, samples were carefully removed from their cast and visually inspected using a stereomicroscope (SteREO Discovery.V12, Zeiss). Specimens that presented air bubbles or imperfections at the boundaries were discarded. Finally, the laboratory models were sprayed with water-based ink to perform digital image correlation (DIC). The use of an air brush enabled us to control with accuracy the speckles sizes (3-5 pixels) and the speckles density (20-40% of the sample surface) (Jones et al. 2018).

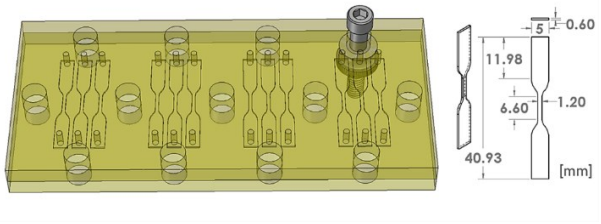

Figure 1. (Left) Representaton of the molding system desinged in Solidworks (Dassault Systemes, v.2018). (Right) Technical drawing of the sample geometry, from the standard ASTM D412-Type C.

TESTING PROTOCOL

We tested the samples using a custom-made micro material testing system equipped with real-time control and acquisition software (LabVIEW, v. 2018, National Instruments). The machine was equipped with a load cell with a capacity of 10N and sensitivity of 10mN. An extensive description of our testing system can be found in (Corti and Shameen et al. 2022). The experiments consisted of applying 10-cylces preconditioning stretch at 10% strain, followed by one-single pull to rupture. The loading cycle was governed by a ramp waveform under displacement control at a constant strain rate of 1.5mm/s. Throughout the test, the reaction force and displacement were measured by the system and images of the sample were recorded by a FLIR Blackfly S high-resolution camera (Teledyne FLIR) equipped with a Tamron M111FM50 lens (IDS Imaging).

DATA PROCESSING

To perform DIC analyses we used the GOM Correlate software (ZEISS Group, v.2019) which allowed us to obtain the True (Cauchy) stress and strain for each sample as well as the material Poisson's ratio, ν. The true stress values were calculated by measuring the reduction in cross-sectional area from the change in width in the gauge region throughout the test, assuming the material as isotropic. The average Poisson's ratio for each formulation was obtained considering the material response up to 10% strain and it was computed as (1):

$$\nu = -\frac{\varepsilon_{trans}}{\varepsilon_{axial}}, \tag{1}$$

where ε_{trans} is the transverse strain (perpendicular to the tensile direction) and ε_{axial} is the axial strain (parallel to the tensile direction). The individual and average true stress and strain curves and the Poisson's ratio were obtained combining the data from the tensile system and the DIC analysis in a custom made MATLAB script. By knowing the nominal (engineering) stress and strain, and the Poisson's ratio, we were also able to determine the constitutive coefficients of the 3-term Ogden model for each tested elastomer formulation. The inverse analysis was carried out using the material evaluation capability in Abaqus (Dassault Systemes, v.2019). The 3-term Ogden constitutive model has been widely used to replicate the hyperelastic behavior of arterial tissues (Schiavone, Zhao, and Abdel-Wahab 2014; Martin 2013; Karimi, Navidbakhsh, and Razaghi 2014; Zahedmanesh and Lally 2009) and it describes the material response to large deformation using the strain energy function given by (2)(Ogden 1997):

$$W = \sum_{i=1}^{3} \frac{\mu_i}{\alpha_i} (\bar{\lambda}_1^{\alpha_i} + \bar{\lambda}_2^{\alpha_i} + \bar{\lambda}_3^{\alpha_i} - 3) + \sum_{i=1}^{3} \frac{1}{D_i} \left(J^{el} - 1\right)^{2i}, \tag{2}$$

where the first term on the right represents the deviatoric part of the elastic strain energy density function and the second term represents the volumetric part. In the equation, $\bar{\lambda}_i$ are the deviatoric principal stretches $\bar{\lambda}_i = J^{-\frac{1}{3}} \lambda_i$, where J is the third invariant of the deformation gradient F, $J = det(\boldsymbol{F}) = \lambda_1 \lambda_2 \lambda_3$;

λ_i are the principal stretches; and α_i are power law coefficients. The initial shear modulus and bulk modulus for the Ogden form are $\mu_0 = \sum_{i=1}^{3} \mu_i$, $K_0 = \frac{2}{D_1}$, respectively. The fitting accuracy of the Ogden description was tested by replicating our experiments in finite element method (FEM) simulations in Abaqus. Each material was considered, and the sample was stretched up to the average ultimate displacement of the corresponding formulation. Finally, the Ogden description was used to simulate the expansion of 30mm-long cylindrical tubes by a uniform and linearly increasing pressure up to 250mmHg. Here, the two axial extremes of the vessels were free to move in the radial direction only. These geometries were designed to replicate the average radius (R=4.15mm) and thickness (H=1.17mm) of common carotid arteries walls reported by Sommer et al.(Sommer et al. 2010)**.**

STATISTICAL ANALYSIS

Data are reported as mean±SD. Analysis of variance was performed by one-way ANOVA test followed by post-hoc pairwise comparison of the mean strength between the groups. The null hypothesis was rejected if $p<0.05$.

Results

TENSILE RESPONSE AND RUPTURE THRESHOLD

The average true stress and strain curves for each group (**Fig. 2**) depict the evident hyperelastic non-linear behavior of the elastomers up to rupture, and the influence that different base to curing agent ratios have on this behavior. Our results show that Sylgard184 is the stiffest of the materials considered as it experiences the highest shear modulus and ultimate stress at relative low strain levels. On the other hand, Sylgard170 and DowsilEE-3200 present significantly lower shear moduli and ultimate stress levels that are closer to data reported for arterial tissues (Holzapfel et al. 2005; Teng et al. 2009). Importantly, Dowsil is the most compliant material, with the lowest shear modulus among these elastomers, and with ultimate stress and strain values very close to arterial tissue. The right panels in **Figure2** offer a closer view of the behavior of each formulation up to a strain of 0.5, which is a common range of stretch in arteries under physiological and supraphysiological loadings.

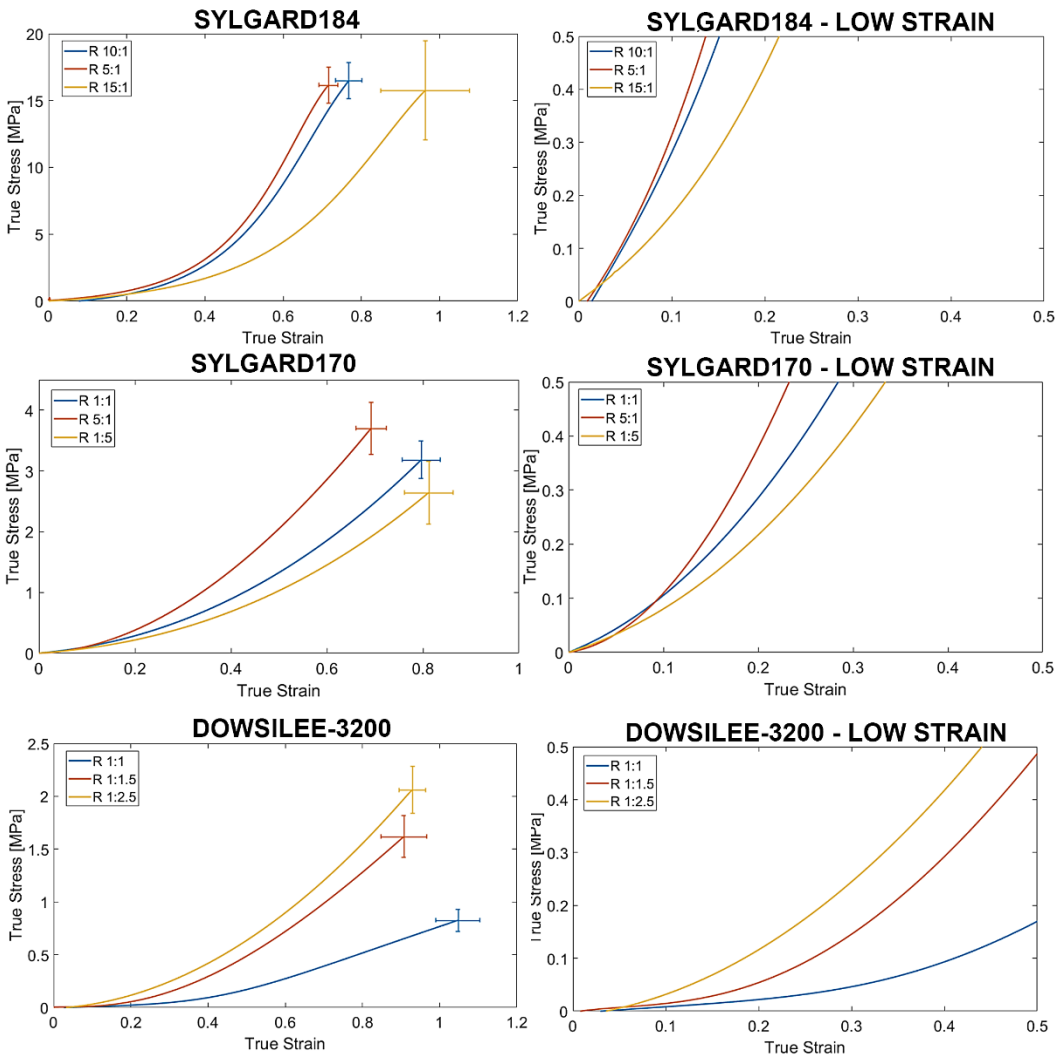

Figure 2. (Left) True stress and strain curves for each mix ratio, with SD error bars at rupture. Top row shows Sylgard 184, Sylgard 170 in the middle row and Dowsil EE-3200 in the bottom row. (Right) True stress and strain curves up to 0.5MPa stress and 0.5 strain. Overall, sylgard 184 is the stiffest elastomer, followed by Sylgard 170 and the most complaint was found to be Dowsil EE-3200. The stress-strain behavior was found tunable (dependent on the polymer to curing agent ratio) in all formulations.

The average ultimate stress and stretch ratio values as well as the Poisson's ratio of each formulation are reported in **Table1.** For comparison purposes, we have also included the longitudinal and circumferential Cauchy stresses and stretch ratios at rupture that have been reported in the literature for carotid and coronary arteries(Teng et al. 2009; Holzapfel et al. 2005). In the first study, Teng et al. analyzed the mechanical behavior under tensile tension of human carotid arteries presenting sections with fatty streak or pre-atheroma with extracellular lipid pools (lesion II-III). The authors were able to test both intact samples as well as dissected media and adventitia layers. In the second study, Holzapfel et al. considered dissected layers intima, media and adventitia of non-stenotic human coronary arteries presenting intimal thickening. Our data show that Sylgard184 is the material with the highest values of ultimate stress, which are far from those showed by human arterial tissues. Differently, Sylgard170 and DowsilEE-3200 experience significantly lower stresses at rupture, with Dowsil having the highest extensibility. The statistical analysis on the effect of mix ratios for each formulation is illustrated in **Figure3**. For Sylgard184, our results indicate similar stresses at rupture among the three formulations, while there is a significant difference between R15:1 ultimate strain and the other two ratios. Reducing the relative amount of curing agent from the

recommended mix ratio increases the extensibility of Sylgard184. In the case of Sylgard170, each ratio presents statistically different ultimate stresses and R5:1 is the only formulation that shows a meaningful shift in strain levels. A higher concentration of PartA makes Sylgard170 stiffer. The influence of the mix ratio is also evident for DowsilEE-3200. Each formulation manifests different stress values at rupture with the amount of PartB being positively correlated to the stress values. The strain deviates only when considering a higher concentration of PartB than the amount recommended by the provider.

Table 1 List of ultimate stress, ultimate strain and Poisson's ratio for each formulation as well as longitudinal (zz) and circumferential (θθ) stress and strain for human arteries reported in the literature.

Material	**Part A:B ratio**	**# of samples (n)**	**Ultimate σ_{true} [MPa]**	**Ultimate λ**	**ν**
Sylgard 184	15:1	11	15.898±3.741	1.963±0.113	0.496±0.007
	10:1	10	16.541±1.450	1.767±0.0340	0.493±0.004
	5:1	8	16.243±1.316	1.716±0.0243	0.492±0.006
Sylgard 170	5:1	10	3.665±0.430	1.692±0.032	0.472±0.005
	1:1	12	3.147±0.310	1.770±0.023	0.463±0.013
	1:5	9	2.607±0.512	1.812±0.051	0.478±0.001
Dowsil EE-3200	1:1	9	0.825±0.102	2.048±0.057	0.491±0.016
	1:1.5	9	1.609±0.195	1.907±0.059	0.490±0.008
	1:2.5	11	2.049±0.220	1.930±0.035	0.481±0.006
Artery	**Tissue**	**Ultimate σ_{zz} [MPa]**	**Ultimate λ_{zz}**	**Ultimate $\sigma_{\theta\theta}$ [MPa]**	**Ultimate $\lambda_{\theta\theta}$**
Human carotid (Teng et al)	Intact	1.570±0.1295	1.50±0.200	1.5637±0.351	1.53±0.270
	Media	0.727±0.52	1.40±0.180	1.8081±1.224	1.47±0.250
	Adventitia	3.074±1.993	1.54±0.230	2.8291±1.655	1.57±0.220
Human coronary (Holzapfel et al)	Intima	0.391±0.144	1.55±0.400	0.394±0.223	1.6±0.290
	Media	0.419±0.188	1.74±0.280	0.446±0.194	1.81±0.370
	Adventitia	1.300±0.692	1.87±0.380	1.430±0.604	1.66±0.240

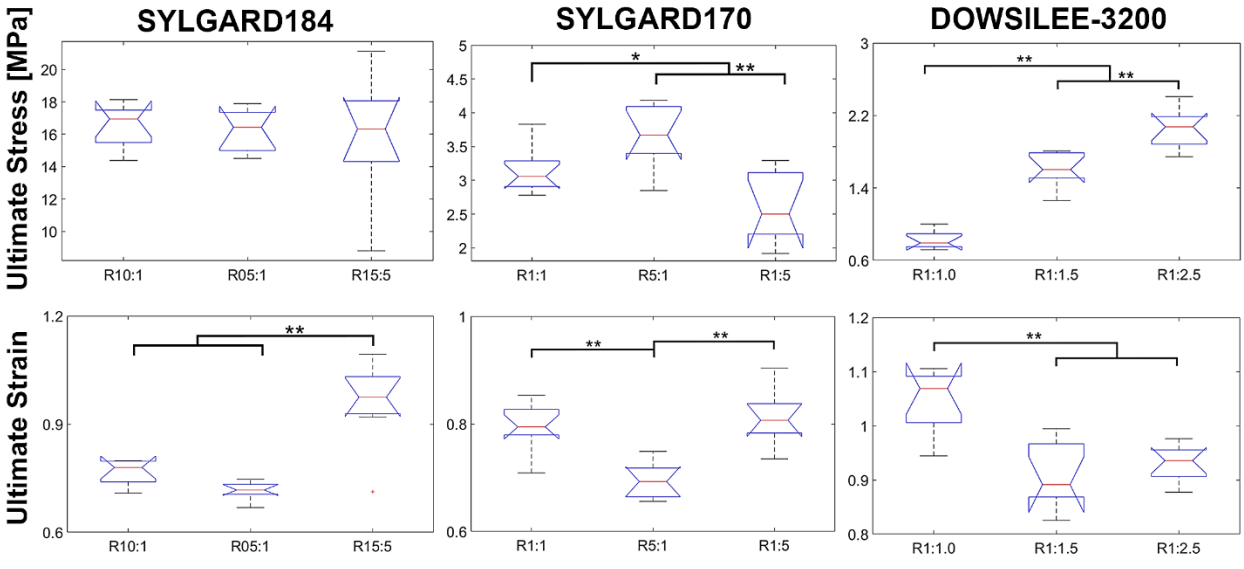

*Figure 3. Boxplots of ultimate stresses and strains for each formulation with the corresponding statistical significance (*p<0.05, **p<<0.05).*

STRESS TO STRETCH RATIO RESPONSE OF LABORATORY MODELS AND ATHEROSCLEROTIC CAROTID TISSUES

To validate the mechanical behavior of our laboratory models, we compared their stress vs stretch ratio (where the stretch ratio λ = strain+1) response to published data of carotid plaques after endarterectomy (Mulvihill et al. 2013; Lawlor et al. 2011; Maher et al. 2009) (**Fig4**). In addition, we included for comparison the tensile test data of one sample of intact atherosclerotic carotid artery from Teng et al. (Teng et al. 2009). In this analysis, we considered the formulation of each material that could better fit the arterial data (Sylgard184 R10:1, Sylgard170 R1:1 and DowsilEE-3200 R1:1.5).

Maher et al. and Lawlor et al. performed uniaxial tensile tests in the circumferential direction on surgically removed carotid plaques. Mulvihill et al. studied carotid plaques specimens under pure shear tests in the circumferential direction. **Figure 4** shows a significant variability between studies as well as within each data set. These large variations may be attributed to different plaque types (i.e calcified, soft or mixed). The stress-stretch ratio curve from Teng et al. presents a higher ultimate stress probably due to the presence of the media and adventitia layers, which are often missing in endarterectomy samples.

Our laboratory models exhibit an axial response that lie within the ranges of carotid tissues. Sylgard184 appears more suited to replicate stiffer behaviors and closely approaches the average curve in Maher et al. Sylgard170 shows a stress-stretch curve that well fits the range reported by Maher et al. and displays similar nonlinear stress and stretch levels to the data from Teng et al. DowsilEE-3200 falls within the stress-stretch ranges of the three studies and better correlates to the data from Lawlor et al. and Mulvihill et al. Our results reveal that each formulation can potentially replicate the mechanical response of carotid tissues before rupture. Indeed, Sylgard 184 and Sylgard 170 could be used for modeling the adventitia and/or the media layer(s) of the laboratory model, but they will not be suited for replicating the rupture of the intima layer due to the significant different ultimate stress and stress levels shown by these materials when compared to blood vessels. However, the only material that is able to reproduce similar ultimate stress and stretch values to rupture of the intima and media layers is DowsilEE-3200, as Sylgard184 and Sylgard170 reaches stress levels that are far beyond the rupture threshold of carotid samples.

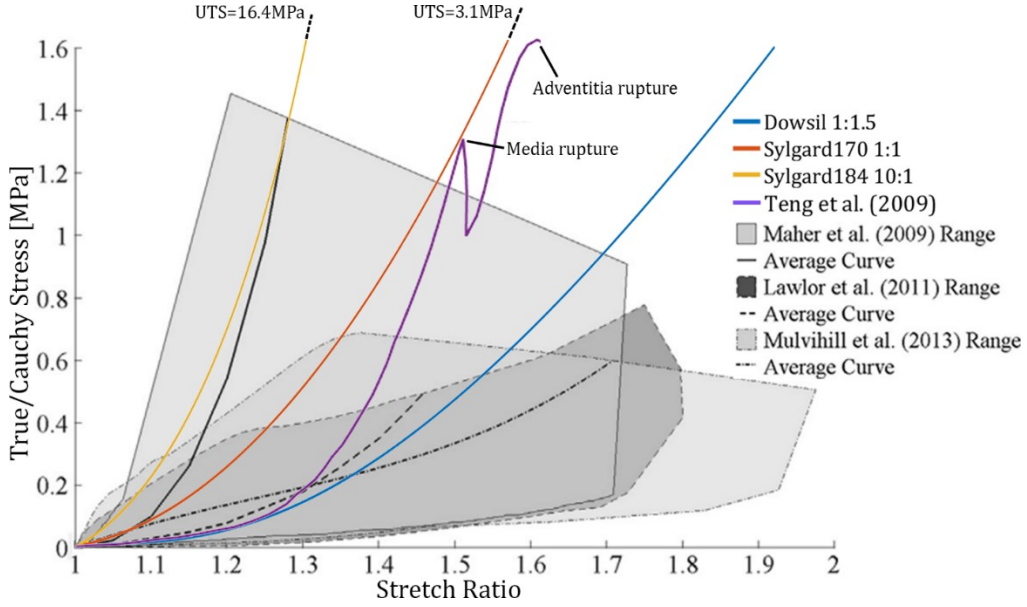

Figure 4. Cauchy stress vs stretch ratio of carotid plaques and intact carotid arteries in the circumferential direction vs True stress vs stretch ratio of Sylgard184 R10:1, Sylgard170 R1:1, DowsilEE-3200 R1:1.5. The ultimate stress (UTS) for Sylgard184 and Sylgad170 was also reported as they exceed the maximum stress limit in the graph. (Adapted from Walsh et al. 2014)

MATERIAL FITTING AND NUMERICAL SIMULATIONS

The nominal stress and strain data as well as the Poisson's ratio of each material were imported into Abaqus and the Ogden coefficients were evaluated. Every formulation respected Ducker's stability criteria (Drucker 1959) for all ranges of tension and compression strains and the coefficients values are reported in **Table2**. After obtaining the constitutive description, we performed numerical simulations on samples with the same geometry as our laboratory models. In these finite element analyses, the samples were stretched until reaching similar levels of ultimate strain as the test data. The axial stress and strain in the gauge region were then exported and graphed against the average stress and strain curves of the corresponding formulation. The fitted Ogden model accurately replicates the mechanical response of all material, as can be seen in **Figure5A**. The strain distribution computed through DIC is also similar when compared with that of FEM models, as shown in **Figure 5B**.

Table 2. List of the constitutive Ogden coefficients obtained from experimental stress-strain data of each formulation of Sylgard184, Sylgard170 and DowsilEE-3200

Formulation	μ_1 (MPa)	μ_2	μ_3	α_1	α_2	α_3	D_1 (MPa^{-1})	$D_{2,3}$
Syl184 10:1	-96.70	50.31	47.27	1.71	2.35	0.98	0.02	0
Syl184 15:1	-46.60	23.20	23.92	1.70	2.15	1.19	0.03	0
Syl184 5:1	-12.94	8.76	5.05	1.94	3.23	-0.81	0.09	0
Syl170 1:1	-3.15	1.78	1.76	-2.67	0.31	-5.83	0.39	0
Syl170 1:5	-15.40	7.21	8.52	-2.03	-0.81	-3.35	0.28	0
Syl170 5:1	-35.02	16.30	19.42	-2.14	-0.93	-3.44	0.16	0
DOW 1:1	-17.78	9.10	8.70	0.85	1.12	0.56	2.43	0
DOW 1:1.5	-41.46	21.08	20.42	-0.18	0.24	-0.63	0.78	0
DOW 1:2.5	-38.39	19.17	19.31	-2.46	-1.73	-3.14	0.80	0

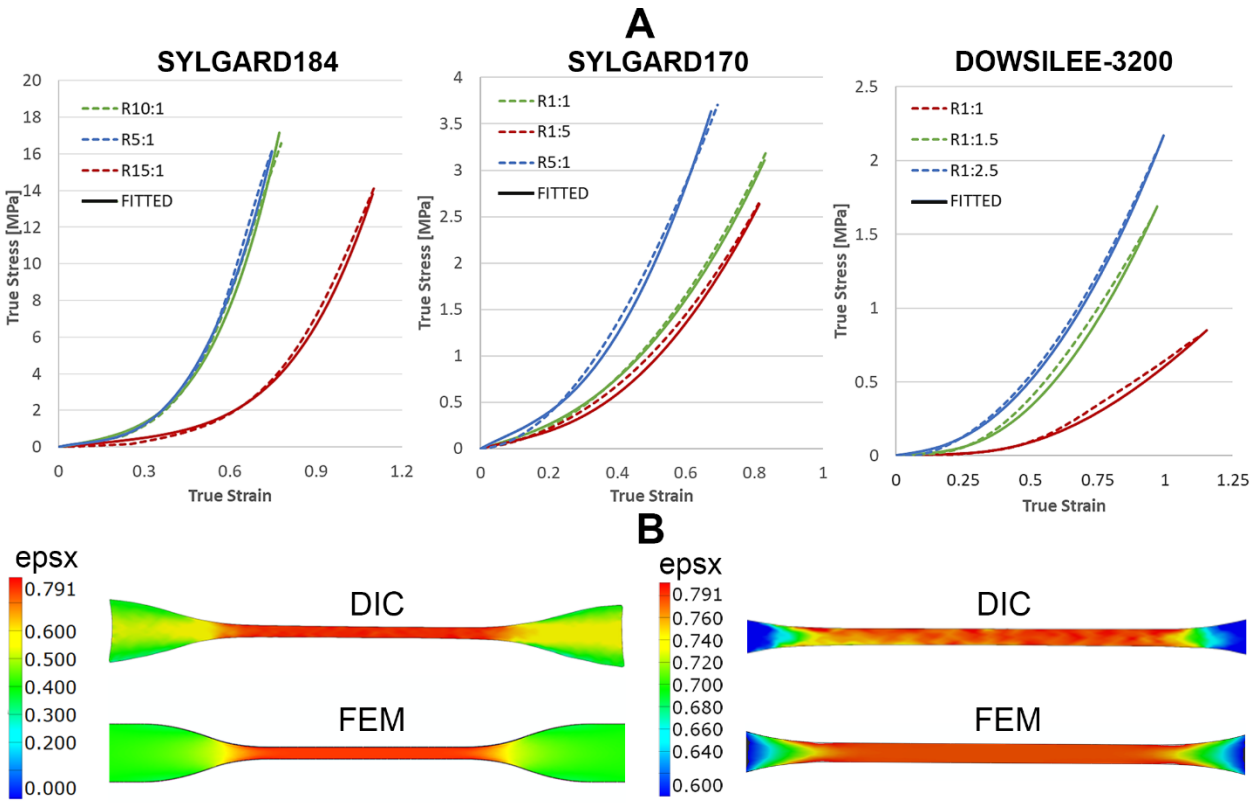

Figure 5. (A). True stress and strain curves of each material and their corresponding numerical model. (B) Comparison of the axial strain (epsx) distribution between the DIC analysis and FEM simulations under the same colour scale on the whole sample (left) and the gauge region (right).

The mechanical behavior of each material under radial pressure is illustrated in **Figure6**, which represents the average values of 30 mesh elements per data set that were selected along the thickness of the vessel. The only formulation that reaches the hyperelastic regime is the Dowsil R1:1, which is the most compliant material considered in this study and undergoes significant degrees of expansion (**Fig6**). It approaches a circumferential stress of 0.5MPa, which corresponds to high levels of strains (0.5-0.9 strain according to Figure 5A). The other materials exhibit similar stress profiles that remain in the elastic region with values that range from 0.1 to 0.18MPa.

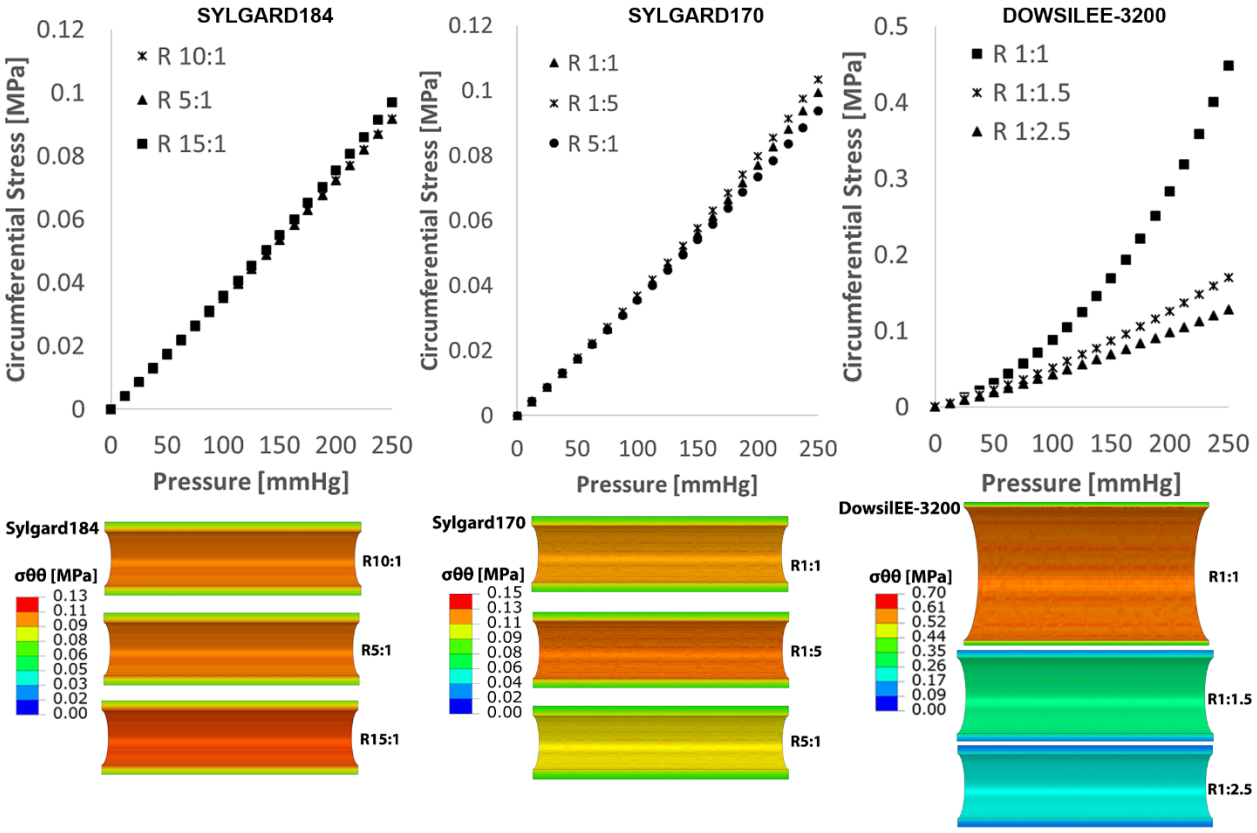

Figure 6. (Top) Stress vs transmural pressure scatter charts for each formulation; (Bottom) Circumferential stress ($\sigma_{\theta\theta}$) distribution on each vessel model. Different color scales were used among Sylgard184, Sylgard170 and DowsilEE-3200.

Discussion

Given Sylgard184 wide range of applications, the tunability of its material properties has been previously studied in terms of morphological features, experimental procedure, curing blends and temperatures. Liu et al. (Liu et al. 2009) documented the effect of the sample thickness on Sylgard184 mechanical properties. The authors demonstrated that a thickness of 200 µm represents the transition point from bulk to thickness-dependent behavior, below which Sylgard184 membranes exhibit 2 to 5-fold increase in stress levels. In this study, we considered 600µm-thick samples and the stress levels that we obtained are close to those reported by Liu et al. for membranes governed by a bulk behavior.

Other researchers have focused on the effect of varying curing temperatures on the mechanical behavior of Sylgard184. Johnston et al. (Johnston et al. 2014) demonstrated that that the material Young's modulus (linear stress-strain behavior at low strains) is directly proportional to the curing temperature, while the maximum strain seems to be inversely proportional to such curing temperature. In the present study, we only focused on one curing temperature for every formulation, but the influence of this factor on Sylgard170 and Dowils EE-3200 might be relevant and worth investigating in the future. In another study, Kim et al. (Kim, Kim, and Jeong 2011) performed uniaxial loadings up to rupture on Sylgard184 samples prepared with different mix ratios. The authors considered blends of 5:1, 10:1 and 15:1 and observed higher stresses and lower strains when increasing the amount of curing agent. The change in strain agrees with what we obtained for ratio 15:1. However, our data show no significant change in ultimate stress regardless of the formulation. We believe this difference originates from the type of stress that is calculated from the raw data. Kim et al. reported the nominal (engineering) stress, which doesn't take into consideration the change in cross-sectional area under stretch, while we were able to derive the True (Cauchy) stress in the sample

making use of the DIC technique.

Different stress measurements and distinct experimental protocols can potentially be the reason why published data for Sylgard184 fluctuate widely among various studies (**Table3**). Indeed, the method used to estimate the strain of the sample gauge region plays a relevant role on the accuracy of the results. In the case of dumbbell-shaped geometries, Schneider et al. (Schneider et al. 2008) showed that the deformation of the shouldered sides of the sample has a significant influence on the total strain progression. The authors calculated that the total strain measured automatically by the tensile machine was more than a factor of 2 larger than the strain in the test section. This difference appears to remain constant up to 40% strain and so it can be addressed by applying a correction factor. However, for larger deformation regimes this assumption is not valid, and the strain of the sample gauge region should be measured directly, either manually or through video elastography.

Table 3. List of stress and strain measurements reported by different studies of Sylgard184 under uniaxial tensile tests. The values listed refer only to formulations that were prepared following the provider's recommendations (mixing ratio 10:1) (ca: circa).

Study	Type of stress	Ultimate stress [MPa]	Strain measurement	Ultimate strain
Mata et al.	Engineering	ca 8	/	/
Liu et al.	Cauchy	ca 25	Logarithmic strain calculated from automatically recorded raw data	ca 140%
Kim et al.	Engineering	ca 1.5	Engineering strain calculated from automatically recorded raw data	ca 160%
Johnston et al.	Engineering	ca 6	Engineering strain calculated from automatically recorded raw data and corrected by a factor of 0.4	ca 110%
Liu et al.	Engineering	ca 9	/	/
Colombo et al.	Engineering	ca 6	Engineering strain from video extensometer	ca 70%
Provider's technical data	Engineering	6.7	/	/

Besides Sylgard184, we extended the analysis of varying curing conditions to Sylgard170 and DowsilEE-3200 which show stress and strain levels much similar to those of arterial tissues. We demonstrated that the mechanical behavior of both materials can be controlled by tuning the amount of the base polymer component and cross-linker. In the case of Sylgar170, the relative amount of PartA appears to govern the stiffness and ultimate strength of the material. For DowsilEE-3200, increasing the PartB concentration leads to higher stresses and lower strains. These results reveal the possibility to adjust the curing ratios of these materials to replicate the mechanical properties of specific vascular tissues or arterial layers (i.e. intima, media and adventitia).

Multiple research groups have studied the anisotropic response of arterial tissues under tensile tests. Their findings vary broadly due to the heterogeneity of the vascular wall, the type of arteries considered and their relative medical history (Holzapfel, Sommer, and Regitnig 2004; Akyildiz, Speelman, and Gijsen 2014; Walsh et al. 2014). We compared our results with the data reported by Teng et al. (Teng et al. 2009) and Holzapfel et al. (Holzapfel, Sommer, and Regitnig 2004) for carotid and coronary arteries, given their relevance in cardiovascular diseases. These reported values from actual anisotropic vascular tissues in the axial and circumferential directions serve as lower and upper reference limits for comparison against our equivalent isotropic laboratory materials. While the isotropic character of elastomers is a limitation when compared to actual anisotropic tissues, isotropic laboratory models are valuable for a broad range of studies in vascular mechanics research. Future studies may extend the use of the Sylgar170 or DowsilEE-3200 with fibers to transform these materials into anisotropic ones. In addition, we focused our attention on the circumferential stresses and strains, as they are often considered as determinants of plaque vulnerability.

Sylgard184 exhibits ultimate stretch ratios that are similar to those of carotid and coronary tissues. However, its ultimate strength is too high when compared with the published human tissue data. Every formulation of this material reaches levels of stresses that offset the ultimate strength of arterial layers by 5-15 times. This difference makes Sylgard184 an inappropriate laboratory model when trying to reproduce the mechanical failure of arterial tissues under similar ranges of stresses and strains.

Sylgard170 also manifests strain levels similar to the data of Teng and Holzapfel. Specifically, ratios 5:1 is the material that most closely approaches the circumferential stretch values of coronary layers. The ultimate stresses are much lower compared to Sylgard184, but they moderately exceed the average values reported for human arteries. However, these levels of stresses appear to lie on the set of values shown by porcine coronary arteries (Lally, Reid, and Prendergast 2004; Noble et al. 2016).

DowsilEE-3200 is the most compliant elastomer in this study. It experiences the lowest values of stresses while reaching higher deformations. For this material, Dowsil 1:1.5 is the formulation that best approaches the stress and strain values of the arteries considered. It shows ultimate stresses that are very close to those of carotid intact wall and layers as well as coronary adventitia. However, the average stretch ratio at rupture lies outside the range of arterial tissues, with values that are up to 40% higher than carotid intact wall samples and 10-30% higher than coronary layers.

From the stress-strain data, we also derived the material constants of the Ogden strain energy function for each formulation. These values can be used to perform numerical studies of different nature, as they guarantee computational stability for all tensile and compressive strains. We used the constitutive description of the materials to investigate the mechanical response of each formulation under radial pressure by means of FEM simulations. We compared the numerical results of our models to those of common carotid arteries studied by Sommer et al. (Sommer et al. 2010). We found that all material but Dowsil 1:1 exhibit a linear increase in stresses up to a pressure of 250mmHg, with maximum values in the range of 100-180kPa. These stresses closely replicate those in (Sommer et al. 2010), which span between 100 and 175kPa depending on the axial pre-stretch. These results demonstrate that cylindrical tubes made of Sylgard184, Sylgard170 and DowsilEE-3200 (except R1:1) undergo similar intramural stress distributions as common carotid arteries under physiological and supraphysiological hydraulic pressures.

Conclusion

In the present study, we performed a mechanical characterization and comparative analysis of three potential vascular tissue mimicking-materials, Sylgard184, Sylgard170 and Dowsil EE-3200 under different composition ratio and curing conditions. The average mechanical behavior for each material was then curve-fitted against a constitutive material description based on the 3-term Ogden hyperelastic model, to obtain the parameters characterizing such constitutive model. Numerical simulations were performed to analyze the behavior of the material in a simplified blood vessel under the action of blood pressure. The tensile behavior to rupture was compared against published data of carotid and coronary arteries. On one hand, we demonstrated that Sylgard184 is significantly stiffer than blood vessels, and highly exceed the ultimate tensile strength shown by these blood vessels. Even though Sylgard184 is among the elastomer materials most commonly used for vascular laboratory models, it does not well replicate the tensile properties to rupture of these tissues. On the other hand, Sylgard170 and DowsilEE-3200 are able to better replicate the typical range of stresses and strains of the arteries being considered. We conclude that Sylgard170 and DowsilEE-3200 are easy to use, mechanically tunable, isotropic elastomer materials that can replicate the hyperelastic behavior to rupture of carotid and coronary arteries, to be used as vascular tissue mimicking laboratory models.

Acknowledgements

Financial support for the conduct of the research was provided by NSF grants CMMI-1662970, MRI-2018485, PSC-CUNY 64696-00 52, and CUNY IRG program. The funding source(s) had no involvement in the study design; in the collection, analysis and interpretation of data; in the writing of the report; and in the decision to submit the article for publication.

Declaration of interest: none

Bibliography

Akyildiz, Ali C., Lambert Speelman, and Frank J H Gijsen. 2014. "Mechanical Properties of Human Atherosclerotic Intima Tissue." *Journal of Biomechanics* 47 (4): 773–83. https://doi.org/10.1016/j.jbiomech.2014.01.019.

Burke, Allen P, Andrew Farb, Gray T Malcom, and John E Smialek. 2014. "Plaque Rupture and Sudden Death Related Artery Disease" 281 (10): 921–26.

Choi, Jung-Yeol, Dae-Woong Park, and Tae Sung Oh. 2014. "Variation of Elastic Stiffness of Polydimethylsiloxane (PDMS) Stretchable Substrates for Wearable Packaging Applications." *Journal of the Microelectronics and Packaging Society* 21 (4): 125–31. https://doi.org/10.6117/kmeps.2014.21.4.125.

Colombo, A., H. Zahedmanesh, D. M. Toner, P. A. Cahill, and C. Lally. 2010. "A Method to Develop Mock Arteries Suitable for Cell Seeding and In-Vitro Cell Culture Experiments." *Journal of the Mechanical Behavior of Biomedical Materials* 3 (6): 470–77. https://doi.org/10.1016/j.jmbbm.2010.04.003.

Corti, Andrea, Tariq Shameen, Shivang Sharma, Annalisa De Paolis, and Luis Cardoso. 2022. "Biaxial Testing System for Characterization of Mechanical and Rupture Properties of Small Samples." *HardwareX* 12: e00333. https://doi.org/10.1016/j.ohx.2022.e00333.

Doyle, Barry J., Aidan J. Cloonan, Michael T. Walsh, David A. Vorp, and Timothy M. McGloughlin. 2010. "Identification of Rupture Locations in Patient-Specific Abdominal Aortic Aneurysms Using Experimental and Computational Techniques." *Journal of Biomechanics* 43 (7): 1408–16. https://doi.org/10.1016/j.jbiomech.2009.09.057.

Doyle, Barry J., Timothy J. Corbett, Aidan J. Cloonan, Michael R. O'Donnell, Michael T. Walsh, David A. Vorp, and Timothy M. McGloughlin. 2009. "Experimental Modelling of Aortic Aneurysms: Novel Applications of Silicone Rubbers." *Medical Engineering and Physics* 31 (8): 1002–12. https://doi.org/10.1016/j.medengphy.2009.06.002.

Drucker, D.C. 1959. "A Definition of Stable Inelastic Material." *J. Appl. Mech.*

Fischer, Sarah C.L., Klaus Kruttwig, Vera Bandmann, René Hensel, and Eduard Arzt. 2017. "Adhesion and Cellular Compatibility of Silicone-Based Skin Adhesives." *Macromolecular Materials and Engineering* 302 (5): 1–11. https://doi.org/10.1002/mame.201600526.

Fratzl, Peter. 2008. *Collagen: Structure and Mechanics*. Edited by Peter Fratzal. Springer, Boston, MA. https://doi.org/https://doi.org/10.1007/978-0-387-73906-9_1.

Hecker, Louise, Keith Baar, Robert G. Dennis, and Khalil N. Bitar. 2005. "Development of a Three-Dimensional Physiological Model of the Internal Anal Sphincter Bioengineered in Vitro from Isolated Smooth Muscle Cells." *American Journal of Physiology - Gastrointestinal and Liver Physiology* 289 (2 52-2): 188–96. https://doi.org/10.1152/ajpgi.00335.2004.

Holzapfel, Gerhard A, Gerhard Sommer, Christian T Gasser, Peter Regitnig, A Gerhard, Gerhard Sommer, Christian T Gasser, and Peter Regitnig. 2005. "Determination of Layer-Specific Mechanical Properties of Human Coronary Arteries with Nonatherosclerotic Intimal

Thickening and Related Constitutive Modeling." *Am J Physiol Heart Circ Physiol* 289: 2048–58. https://doi.org/10.1152/ajpheart.00934.2004.

Holzapfel, Gerhard A, Gerhard Sommer, and Peter Regitnig. 2004. "Anisotropic Mechanical Properties of Tissue Components in Human Atherosclerotic Plaques." *Journal of Biomechanical Engineering* 126 (5): 657–65. https://doi.org/10.1115/1.1800557.

Jankowska, Malgorzata A., Magdalena Bartkowiak-Jowsa, and Romuald Bedzinski. 2015. "Experimental and Constitutive Modeling Approaches for a Study of Biomechanical Properties of Human Coronary Arteries." *Journal of the Mechanical Behavior of Biomedical Materials* 50: 1–12. https://doi.org/10.1016/j.jmbbm.2015.05.021.

Johnston, I D, D K McCluskey, C K L Tan, and M C Tracey. 2014. "Mechanical Characterization of Bulk Sylgard 184 for Microfluidics and Microengineering." *J. Micromech. Microeng.* 24 (3). https://doi.org/10.1088/0960-1317/24/3/035017.

Jones, Elizabeth M C, Mark A Iadicola, Rory Bigger, Benoît Blaysat, Christofer Boo, Manuel Grewer, Jun Hu, et al. 2018. "A Good Practices Guide for Digital Image Correlation." *International Digital Image Correlation Society*, 94.

Karimi, Alireza, Mahdi Navidbakhsh, and Reza Razaghi. 2014. "A Finite Element Study of Balloon Expandable Stent for Plaque and Arterial Wall Vulnerability Assessment." *Journal of Applied Physics* 116 (4). https://doi.org/10.1063/1.4891019.

Kim, Tae Kyung, Jeong Koo Kim, and Ok Chan Jeong. 2011. "Measurement of Nonlinear Mechanical Properties of PDMS Elastomer." *Microelectronic Engineering* 88 (8): 1982–85. https://doi.org/10.1016/j.mee.2010.12.108.

Kural, Mehmet H., Mingchao Cai, Dalin Tang, Tracy Gwyther, Jie Zheng, and Kristen L. Billiar. 2012. "Planar Biaxial Characterization of Diseased Human Coronary and Carotid Arteries for Computational Modeling." *Journal of Biomechanics* 45 (5): 790–98. https://doi.org/10.1016/j.jbiomech.2011.11.019.

Kyriacos, Deny. 2017. "High-Temperature Engineering Thermoplastics." *Brydson's Plastics Materials: Eighth Edition*, 545–615. https://doi.org/10.1016/B978-0-323-35824-8.00021-9.

Lally, C., A. J. Reid, and Patrick J. Prendergast. 2004. "Elastic Behavior of Porcine Coronary Artery Tissue under Uniaxial and Equibiaxial Tension." *Annals of Biomedical Engineering* 32 (10): 1355–64. https://doi.org/10.1114/B:ABME.0000042224.23927.ce.

Lawlor, Michael G., Michael R. O'Donnell, Barry M. O'Connell, and Michael T. Walsh. 2011. "Experimental Determination of Circumferential Properties of Fresh Carotid Artery Plaques." *Journal of Biomechanics* 44 (9): 1709–15. https://doi.org/10.1016/j.jbiomech.2011.03.033.

Liu, Miao. 2007. "Characterization Study of Bonded and Unbonded Polydimethylsiloxane Aimed for Bio-Micro-Electromechanical Systems-Related Applications." *Journal of Micro/Nanolithography, MEMS, and MOEMS* 6 (2): 023008. https://doi.org/10.1117/1.2731381.

Liu, Miao, Jianren Sun, and Quanfang Chen. 2009. "Influences of Heating Temperature on Mechanical Properties of Polydimethylsiloxane." *Sensors and Actuators, A: Physical* 151

(1): 42–45. https://doi.org/10.1016/j.sna.2009.02.016.

Liu, Miao, Jianren Sun, Ying Sun, Christopher Bock, and Quanfang Chen. 2009. "Thickness-Dependent Mechanical Properties of Polydimethylsiloxane Membranes." *Journal of Micromechanics and Microengineering* 19 (3). https://doi.org/10.1088/0960-1317/19/3/035028.

Macrae, R. A., K. Miller, and B. J. Doyle. 2016. "Methods in Mechanical Testing of Arterial Tissue: A Review." *Strain* 52 (5): 380–99. https://doi.org/10.1111/str.12183.

Maher, Eoghan, Arthur Creane, Sherif Sultan, Niamh Hynes, Caitríona Lally, and Daniel J. Kelly. 2009. "Tensile and Compressive Properties of Fresh Human Carotid Atherosclerotic Plaques." *Journal of Biomechanics* 42 (16): 2760–67. https://doi.org/10.1016/j.jbiomech.2009.07.032.

Martin, David. 2013. "Finite Element Analysis of Balloon-Expandable Coronary Stent Deployment : Influence of Angioplasty Balloon Configuration," 1161–75. https://doi.org/10.1002/cnm.2557.

Mata, Alvaro, Aaron J. Fleischman, and Shuvo Roy. 2005. "Characterization of Polydimethylsiloxane (PDMS) Properties for Biomedical Micro/Nanosystems." *Biomedical Microdevices* 7 (4): 281–93. https://doi.org/10.1007/s10544-005-6070-2.

Mulvihill, J. J., E. M. Cunnane, S. M. McHugh, E. G. Kavanagh, S. R. Walsh, and M. T. Walsh. 2013. "Mechanical, Biological and Structural Characterization of in Vitro Ruptured Human Carotid Plaque Tissue." *Acta Biomaterialia* 9 (11): 9027–35. https://doi.org/10.1016/j.actbio.2013.07.012.

Noble, Christopher, Nicole Smulders, Nicola H. Green, Roger Lewis, Matt J. Carré, Steve E. Franklin, Sheila MacNeil, and Zeike A. Taylor. 2016. "Creating a Model of Diseased Artery Damage and Failure from Healthy Porcine Aorta." *Journal of the Mechanical Behavior of Biomedical Materials* 60: 378–93. https://doi.org/10.1016/j.jmbbm.2016.02.018.

Ogden, Ray W. 1997. *Non-Linear Elastic Deformations*. Dover Publications.

Payan, Yohan, and Jacques Ohayon. 2017. *Biomechanics of Living Organs*. *Biomechanics of Living Organs*. 1st ed. Elsevier. https://doi.org/10.1016/c2015-0-00832-2.

Roth, Gregory A., George A. Mensah, Catherine O. Johnson, Giovanni Addolorato, Enrico Ammirati, Larry M. Baddour, Noel C. Barengo, et al. 2020. "Global Burden of Cardiovascular Diseases and Risk Factors, 1990-2019: Update From the GBD 2019 Study." *Journal of the American College of Cardiology* 76 (25): 2982–3021. https://doi.org/10.1016/j.jacc.2020.11.010.

Schiavone, A., L. G. Zhao, and A. A. Abdel-Wahab. 2014. "Effects of Material, Coating, Design and Plaque Composition on Stent Deployment inside a Stenotic Artery - Finite Element Simulation." *Materials Science and Engineering C* 42: 479–88. https://doi.org/10.1016/j.msec.2014.05.057.

Schneider, F., T. Fellner, J. Wilde, and U. Wallrabe. 2008. "Mechanical Properties of Silicones for MEMS." *Journal of Micromechanics and Microengineering* 18 (6). https://doi.org/10.1088/0960-1317/18/6/065008.

Sommer, Gerhard, Peter Regitnig, Lukas Költringer, and Gerhard A. Holzapfel. 2010. "Biaxial Mechanical Properties of Intact and Layer-Dissected Human Carotid Arteries at Physiological and Supraphysiological Loadings." *American Journal of Physiology - Heart and Circulatory Physiology* 298 (3): 898–912. https://doi.org/10.1152/ajpheart.00378.2009.

Teng, Zhongzhao, Dalin Tang, Jie Zheng, Pamela K. Woodard, and Allen H. Hoffman. 2009. "An Experimental Study on the Ultimate Strength of the Adventitia and Media of Human Atherosclerotic Carotid Arteries in Circumferential and Axial Directions." *Journal of Biomechanics* 42 (15): 2535–39. https://doi.org/10.1016/j.jbiomech.2009.07.009.

Walsh, M. T., E. M. Cunnane, J. J. Mulvihill, A. C. Akyildiz, F. J.H. Gijsen, and G. A. Holzapfel. 2014. "Uniaxial Tensile Testing Approaches for Characterisation of Atherosclerotic Plaques." *Journal of Biomechanics* 47 (4): 793–804. https://doi.org/10.1016/j.jbiomech.2014.01.017.

World Health Organization. 2020. "Global Health Estimates for 2020: Deaths by Cause, Age, Sex, by Country and by Region, 2000-2019." *Who*, no. December: 1–59. https://www.who.int/data/gho/data/themes/mortality-and-global-health-estimates/ghe-leading-causes-of-death.

Zahedmanesh, Houman, and Caitríona Lally. 2009. "Determination of the Influence of Stent Strut Thickness Using the Finite Element Method: Implications for Vascular Injury and in-Stent Restenosis." *Medical and Biological Engineering and Computing* 47 (4): 385–93. https://doi.org/10.1007/s11517-009-0432-5.